Essentially Entropic Lattice Boltzmann Model

Mohammad Atif,[1] Praveen Kumar Kolluru,[1] Chakradhar Thantanapally,[2] and Santosh Ansumali[1,2,*]

[1]*Engineering Mechanics Unit, Jawaharlal Nehru Centre for Advanced Scientific Research, Jakkur, Bangalore 560064, India*

[2]*SankhyaSutra Labs Private Limited, Bangalore 560064, India*

(Received 17 May 2017; published 14 December 2017)

The entropic lattice Boltzmann model (ELBM), a discrete space-time kinetic theory for hydrodynamics, ensures nonlinear stability via the discrete time version of the second law of thermodynamics (the H theorem). Compliance with the H theorem is numerically enforced in this methodology and involves a search for the maximal discrete path length corresponding to the zero dissipation state by iteratively solving a nonlinear equation. We demonstrate that an exact solution for the path length can be obtained by assuming a natural criterion of negative entropy change, thereby reducing the problem to solving an inequality. This inequality is solved by creating a new framework for construction of Padé approximants via quadrature on appropriate convex function. This exact solution also resolves the issue of indeterminacy in case of nonexistence of the entropic involution step. Since our formulation is devoid of complex mathematical library functions, the computational cost is drastically reduced. To illustrate this, we have simulated a model setup of flow over the NACA-0012 airfoil at a Reynolds number of 2.88×10^6.

DOI: 10.1103/PhysRevLett.119.240602

The lattice Boltzmann model (LBM) is an efficient kinetic formulation of nonlinear hydrodynamic phenomena in terms of a discrete set of populations restricted on lattices with appropriate symmetries [1–11]. The Navier-Stokes dynamics emerges from this kinetic model by an appropriate choice of discrete equilibrium that respects macroscopic constraints [12–16]. Historically, the approach of choosing the equilibrium from macroscopic dynamics in the LBM emerged as a computationally attractive alternative to the Boolean particle dynamics of the lattice gas model [12–14,17,18]. However, this top-down approach of the LBM lost many desirable features of the lattice gas such as the H theorem and consequently the faithful representation of microscopic Boltzmann dynamics [2,3]. The absence of discrete time H-theorem results in the growth of numerical instabilities in standard LBM. This often makes simulations with low viscosity and/or large spatial gradients for hydrodynamics and large density ratios for multiphase flows unstable [2,3,5].

The entropic lattice Boltzmann model (ELBM) restores the H theorem for discrete space-time evolution [2,3,19–24]. Its introduction was a paradigm shift for computational fluid dynamics where the numerical stability of a hydrodynamic solver was enforced by insisting on adherence to the thermodynamics at the discrete time level [3]. The H theorem in the ELBM requires an additional step of numerically searching for the maximal discrete path length which corresponds to a jump to a mirror state on the isoentropic surface (zero dissipation state). Considerable efforts have been made to ensure the correctness and efficient implementation of this step [25–29]. However, there is scope for better theoretical understanding of the solution provided by the ELBM. For example, an implicit modeling of unresolved scales of the flow, via the thermodynamic route, may provide a new insight into subgrid modeling of turbulence. Such an understanding will also help enhance the efficiency of the ELBM and resolve ambiguities in its implementation. For the rare events when the isoentropic surfaces are partially outside the polytope of positivity, the entropic involution step has no solution and, hence, there is no unique definition of the path length [29].

In this Letter, we reformulate the ELBM and obtain a closed form analytic solution for the discrete path length. The essential idea is to relax the entropy equality condition used in the ELBM and replace it with the constraint that entropy must increase within a discrete time step. We show that near equilibrium this exact solution reduces to the standard LBM. The simplicity of the exact solution removes the computational overhead and algorithmic complexity associated with the ELBM.

Before presenting our exact solution, we present a brief review of the LBM and its entropic formulation in D dimensions. In the LBM, one defines a set of discrete velocities $\mathbf{c}_i$, $i = 1, \ldots, N$ such that they form links of a space-filling lattice [1] and at every lattice node $\mathbf{x}$ and time t a set of discrete populations $f(\mathbf{c}_i, \mathbf{x}, t) \equiv f_i$. We also define the inner product between two functions of discrete velocities ϕ and ψ as $\langle \phi, \psi \rangle = \sum_{i=1}^{N} \phi_i \psi_i$. The hydrodynamic variables such as the mass density ρ, velocity $\mathbf{u}$, and the temperature T are defined as

$$\rho = \langle f, 1 \rangle, \qquad \rho \mathbf{u} = \langle f, \mathbf{c} \rangle, \qquad \rho u^2 + D\rho R T = \langle f, \mathbf{c}^2 \rangle, \tag{1}$$

where R is the gas constant. The evolution for populations after a time step Δt is written as a two-step process of discrete free flight $f_i(\mathbf{x}+\mathbf{c}_i\Delta t, t+\Delta t) = f_i^*(\mathbf{x},t)$ and the collisional relaxation towards discrete equilibrium often modeled by a single relaxation model of Bhatnagar, Gross, and Krook (BGK) [30] with mean free time τ as

$$f_i^*(\mathbf{x},t) = f_i(\mathbf{x},t) + \alpha\beta[f_i^{\mathrm{eq}}(\mathbf{x},t) - f_i(\mathbf{x},t)], \quad (2)$$

where the path length $\alpha = 2$ and $\beta = \Delta t/(2\tau + \Delta t)$ is a dimensionless parameter bounded in the interval $0 < \beta < 1$ ($\beta = 1$ is the dissipationless state). The local equilibrium distribution f_i^{eq} is a minimizer of the convex entropy function H, typically taken in Boltzmann form [2,20,31] $H(f) = \langle f, (\log(f/w) - 1)\rangle$, with weights $w_i > 0$ under the constraint that the mass density, the momentum density, and the energy density (ignored in isothermal models) are fixed [2,20,31]. In this Letter, exact equilibrium is found numerically at every grid point.

The ELBM introduces the concept of state-dependent path length α for the discrete collision step [2]. The dependence on the local state is introduced in terms of the equal entropy mirror state $f^{\mathrm{mirror}} = f + \alpha(f^{\mathrm{eq}} - f)$, which is found by iteratively solving the nonlinear equation [25,26]

$$H(f^{\mathrm{mirror}}) = H(f). \quad (3)$$

Figure 1 shows that beyond the f^{mirror} state H increases along the collision path and thus α corresponds to the maximal path length. The H theorem for the discrete dynamics, $H(f^*) < H(f)$, is ensured by searching point f^{mirror} as $\beta < 1$. In a well-resolved simulation, the dimensionless departure from the equilibrium $x_i = (f_i^{\mathrm{eq}} - f_i)/f_i$ is small ($|x_i| \ll 1$). Hence, Eq. (3) simplifies to $H(f^{\mathrm{mirror}}) - H(f) = \langle f, (1+\alpha x)\log(1+\alpha x)\rangle - \alpha\langle f, x\log(1+x)\rangle$. Expanding the logarithms about $x_i = 0$ using Taylor series one obtains $H(f^{\mathrm{mirror}}) - H(f) = \alpha(\alpha/2 - 1)\langle f, x^2\rangle + O(x^3)$. Thus, close to equilibrium, the nontrivial root for $H(f^{\mathrm{mirror}}) = H(f)$ is $\alpha = 2$, which corresponds to the standard LBM.

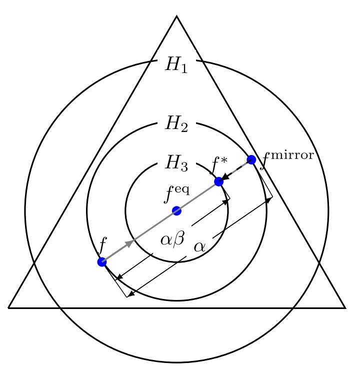

FIG. 1. The entropic involution step: H_i are different entropy levels ($H_1 > H_2 > H_3$). Triangle denotes the polytope of positivity. Note that the precollisional state f and the mirror state f^{mirror} are at the same entropy level. The postcollisional state f^* is at a lower entropy level.

Finally, we note that the involution step has no solution when the isoentropic surfaces are partially outside the polytope of positivity (entropy level H_1 in Fig. 1) [29].

We now present an alternate construction of the ELBM where the discrete path length α has no indeterminacy. The key idea is to obtain α by directly considering the natural criterion of monotonic decrease of the H-functional with time. This implies solving an inequality

$$\Delta H \equiv H(f^*) - H(f) \le 0, \quad (4)$$

which using Eq. (2) is rewritten as

$$\Delta H \equiv \langle f, (1+\hat{\alpha}x)\log(1+\hat{\alpha}x) - \hat{\alpha}x\log(1+x)\rangle, \quad (5)$$

where $\hat{\alpha} = \alpha\beta$. The inequality, by construction, accepts multiple solutions. For example, when $\alpha \le 1$ the inequality is trivially satisfied as the new state is a convex combination of the old state and the equilibrium [23]. However, one is interested in over-relaxed collision, where the new state is no longer a convex combination of the old state and equilibrium. This corresponds to the real solutions of Eq. (4) in the range $1 < \alpha < \infty$ [2]. As in the ELBM, the solution should reduce to the standard LBM close to equilibrium ($\alpha = 2$). Indeed, the present methodology is valid for both discrete velocity models of the LBM as well as the continuous in velocity Boltzmann-BGK equations, where the summation in the inner products needs to be replaced by appropriate integrals.

In order to find $\alpha^{\max}$ that satisfies $\Delta H \le 0$, we need to provide bounds on $\log(1+y)$. For $y \in (-1, 0)$ we consider the Taylor series of $\log(1+y) = \sum_{k=1}^{\infty}(-1)^{k+1}y^k/k$ where each term of the series is negative, hence, any finite truncation will be larger than $\log(1+y)$, i.e.,

$$\log(1+y) < \sum_{k=1}^{N}(-1)^{k+1}\frac{y^k}{k}. \quad (6)$$

In the subsequent lines, we point out certain lesser known inequalities pertaining to $\log(1+y)$ and its Padé approximants. A crucial insight at this point comes from understanding Padé approximants of $\log(1+y)$ as approximate integral $\int_0^y F(z)dz$, where $F(z) = 1/(1+z)$. The integral is approximated via Newton-Cotes (NC) and Gauss-Legendre (GL) quadrature which allows us to provide bounds on $\log(1+y)$ as the related residues are well understood. From nth order Newton-Cotes quadrature $\int_0^y F(z) = \mathcal{I}_{\mathrm{NC}}^{(n)}(y) - p_1 F^{(2n)}(\xi)$ and from Gauss-Legendre quadrature $\int_0^y F(z) = \mathcal{I}_{\mathrm{GL}}^{(n)}(y) + p_2 F^{(2n)}(\xi)$ where p_1, p_2 are positive and $F^{(2n)}(\xi)$ is $2n$th derivative of $F(z)$ at a point ξ inside the domain [$F^{(2n)}(\xi) > 0$ owing to the convex nature of $F(z)$]. Figure 2 shows that for the Newton-Cotes quadrature the residues are positive and their magnitude progressively decreases with an increase in the order of quadrature. The

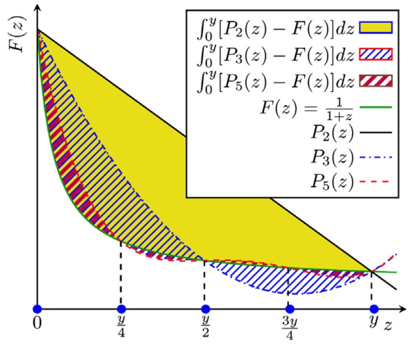

FIG. 2. Residue related to the approximations of $\log(1+y)$ evaluated with the trapezoid rule, $\frac{1}{3}$ Simpson's rule, Boole rule, i.e., the first-, second-, and third-order Newton-Cotes quadratures, respectively. Here P_n are the integrating polynomials. The residues are positive and their magnitude progressively decreases with increase in the order of quadrature.

same can be said about the Gauss-Legendre quadrature, where the residues are negative.

The first-order approximations form the Hermite-Hadamard inequality

$$F\left(\frac{y}{2}\right) \leq \frac{1}{y}\int_0^y F(z)dz \leq \frac{1}{2}[F(0) + F(y)], \qquad (7)$$

where the latter inequality is a consequence of the trapezoid rule (see Fig. 2) and the former is proved using convexity arguments in the Supplemental Material [32]. Stricter bounds on $\log(1+y)$ are constructed by approximating via higher-order quadratures, hence, we obtain an extended version of the Hermite-Hadamard inequality for $y \in [0, \infty)$

$$\mathcal{I}^{(1)}_{\mathrm{GL}}(y) \leq \mathcal{I}^{(3)}_{\mathrm{GL}}(y) \leq \log(1+y) \leq \mathcal{I}^{(3)}_{\mathrm{NC}}(y) \leq \mathcal{I}^{(1)}_{\mathrm{NC}}(y), \qquad (8)$$

where $\mathcal{I}^{(1)}_{\mathrm{NC}}(y) = (y + y^2/2)/(1+y)$, $\mathcal{I}^{(1)}_{\mathrm{GL}}(y) = 2y/(2+y)$, $\mathcal{I}^{(3)}_{\mathrm{NC}}(y) = [7y + 128y/(4+y) + 48y/(4+2y) + 128y/(4+3y) + 7y/(1+y)]/90$, $\mathcal{I}^{(3)}_{\mathrm{GL}}(y) = (60y + 60y^2 + 11y^3)/(60 + 90y + 36y^2 + 3y^3)$.

To find the exact solution, we further introduce a decomposition of distributions f in terms of the departure from equilibrium as $\Omega^+ = \{f_i : x_i \geq 0\}$ and $\Omega^- = \{f_i : -1 < x_i < 0\}$ [33]. The lower bound of x_i in Ω^- comes from the limiting case of the total mass being localized to one particular f_i, whereas the requirement of positivity implies $f_i^{\mathrm{eq}} \geq 0$. This asymmetry of the range of x is crucial in the subsequent derivation of the exact solution. With this decomposition, we also partition the inner product into two partial contributions $\langle f, \psi \rangle_{\Omega^\pm} = \sum_{f_i \in \Omega^\pm} f_i \psi_i$.

Using the proposed decomposition and the mentioned inequalities, Eq. (5) is modified to

$$\Delta H = -\langle f, G_1(\hat{\alpha}x)\rangle_{\Omega^-} - \langle f, G_2(\hat{\alpha}x)\rangle_{\Omega^+} - \hat{\alpha}\langle f, G_3(x)\rangle + \alpha\hat{\alpha}(\beta - 1)\left[\left\langle f, \frac{x^2}{2}\right\rangle - (\hat{\alpha} + \alpha)\left\langle f, \frac{x^3}{2}\right\rangle_{\Omega^-}\right] + \hat{\alpha}\{[\langle f, G_4(x)\rangle_{\Omega^+} + \langle f, G_5(x)\rangle_{\Omega^-}]\}, \qquad (9)$$

where $G_1(y) = -(1+y)\log(1+y) + (y + y^2/2 - y^3/2)$, $G_2(y) = (1+y)[-\log(1+y) + \mathcal{I}^{(1)}_{\mathrm{NC}}(y)]$, and $G_3(y) = y[\log(1+y) - \mathcal{I}^{(1)}_{\mathrm{GL}}(y)]$ are positive semidefinite functions in their respective domains due to Eqs. (6), (8), and $G_4(y) = \alpha y^2/2 - 2y^2/(2+y)$, $G_5(y) = -\alpha^2 y^3/2 + \alpha y^2/2 - 2y^2/(2+y)$. In Eq. (9), all terms are negative except the term in curly brackets. We ensure $\Delta H \leq 0$ by solving the quadratic $g_1(\alpha) = \langle f, G_4(x)\rangle_{\Omega^+} + \langle f, G_5(x)\rangle_{\Omega^-}$ formed by the term in curly brackets, whose positive root α_1 is found as

$$\alpha_1 = \frac{\langle f, x^2\rangle - \sqrt{\langle f, x^2\rangle^2 - 8\langle f, x^3\rangle_{\Omega^-}\langle f, \frac{2x^2}{2+x}\rangle}}{2\langle f, x^3\rangle_{\Omega^-}}. \qquad (10)$$

It can be seen that $\lim_{x_i \to 0}\alpha_1 = 2$. For the purpose of illustration, we simulate the setup of the one-dimensional shock tube, for which the complexity associated with the nonexistent path length for rare events is well understood in the context of ELBM [29]. Flow profiles shown in Fig. 3 illustrate that numerical oscillations are sharply reduced (but not removed) and numerical dissipation is prominent only near points of sharp gradients. Figure 4 shows departure of α from 2 (LBM value) only in a narrow region of sharp gradients (compressive shock front). The above scheme is too dissipative for hydrodynamic applications as at the point of maximum departure the deviation of α from 2 is 11%.

We now construct a less dissipative scheme by considering the stricter inequalities from Eq. (8), using which Eq. (5) is modified to

$$\Delta H = -\langle f, G_6(\hat{\alpha}x)\rangle_{\Omega^-} - \langle f, G_7(\hat{\alpha}x)\rangle_{\Omega^+} - \hat{\alpha}\langle f, G_8(x)\rangle + \langle f, (1 + \hat{\alpha}x)\mathcal{I}^{(3)}_{\mathrm{NC}}(\hat{\alpha}x)\rangle_{\Omega^+} + \langle f, (1 + \hat{\alpha}x)G_9(\hat{\alpha}x)\rangle_{\Omega^-} - \hat{\alpha}\langle f, x\mathcal{I}^{(3)}_{\mathrm{GL}}(x)\rangle, \qquad (11)$$

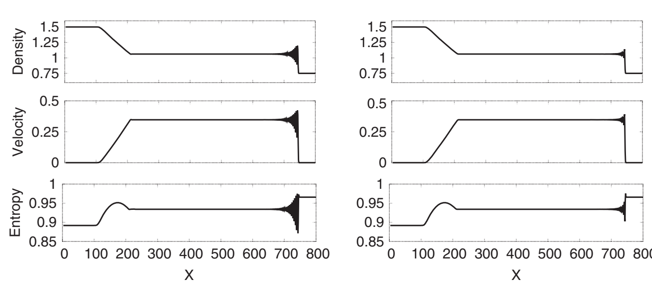

FIG. 3. Density, velocity, and entropy plots from the BGK model, i.e., $\alpha = 2$ (left column), Eq. (10) (right column) at time $t = 500$ for viscosity $\nu = 1.0 \times 10^{-5}$. At $t = 0$, domain was initialized with step density as $\rho(x < 0) = 1.5$ in the left half of domain and $\rho(x > 0) = 0.75$.

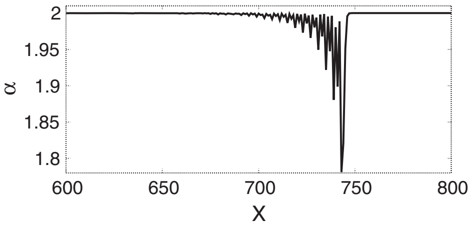

FIG. 4. Snapshot of α at the compressive shock front from Eq. (10) for the shock tube simulation.

where $G_6(y) = (1+y)[-\log(1+y) + G_9(y)]$, $G_7(y) = (1+y)[-\log(1+y) + \mathcal{I}^{(3)}_{\rm NC}(y)]$, $G_8(y) = y[\log(1+y) - \mathcal{I}^{(3)}_{\rm GL}(y)]$ are positive semidefinite in their respective domains due to Eqs. (6), (8), and $G_9(y) = y - y^2/2 + y^3/3 - y^4/4 + y^5/5$. The terms containing G_6, G_7, and G_8 in Eq. (11) are negative definite. The last three terms form an equation in α which can be solved using any iterative scheme. To preserve the computational efficiency, we convert it to a quadratic by solving for $\alpha \in (k, h)$,

$$g(\alpha) = -\alpha^2\beta^2\left\langle f, \frac{x^3}{6} - \frac{h\beta x^4}{12} + \frac{h^2\beta^2 x^5}{20} - \frac{h^3\beta^3 x^6}{5}\right\rangle_{\Omega^-} + \alpha\left[\left\langle f, \frac{x^2}{2}\right\rangle - \left\langle f, \frac{2k\beta^2 x^3}{15}\left(\frac{2}{4+kx} + \frac{1}{4+2kx} + \frac{2}{4+3kx}\right)\right\rangle_{\Omega^+}\right] - \left\langle f, \frac{60x^2 + 60x^3 + 11x^4}{60 + 90x + 36x^2 + 3x^3}\right\rangle. \tag{12}$$

To prove the existence of $\alpha \in (k, h)$ we consider α_2, the root of $g(\alpha)|_{h=0}$ and α_1 from Eq. (10). It can be shown that $g(\alpha_1) < 0 < g(\alpha_2)$ hence a root of $g(\alpha)$ exists in (α_1, α_2). Therefore, the lower bound k is taken as α_1 and the upper bound h is taken as α_2. A detailed proof can be found in the Supplemental Material [32].

As this method inherits the nonlinear stability of the ELBM and provides significant speedup for entropic solvers, model-free simulations of turbulence or multiphase flows for complex scientific and engineering applications with existing computational resources become a distinct possibility. Flow over aerodynamic geometries at a realistic Reynolds number is considered a challenging problem due to the complex turbulence phenomena involved and high resolution required to capture the flow properties [34]. To this effect, simulation of viscous flow over a NACA-0012 airfoil at 10° angle of attack (AOA) and a Reynolds number 2.88×10^6 is performed using a higher-order crystallographic LBM [11] (details of the model and setup will be presented in a separate manuscript). For this setup, the results obtained using $h = 2.05$ are indistinguishable from that obtained by the proposed upper bound. Figure 5(a) shows the coefficient of pressure (C_p) compared with experiment [35] and Fig. 5(b) shows a snapshot of instantaneous vorticity field of an airfoil in stall. To the best of our knowledge this is the first place where turbulence model free simulation is performed at such a high Reynolds number.

To conclude, we say that this new exact solution is a significant step in the theoretical development of the ELBM. Furthermore, this essentially entropic LBM provides an important first step in providing a statistical mechanics route to subgrid scale modeling. For example, using discrete entropic space-time dynamics for Boltzmann BGK equation, we can show that the correction to viscosity is ν_T is (see Supplemental Material for details [32])

$$\nu_T = -\tau\theta \frac{\Delta t}{2} \frac{S_{ij}S_{jk}S_{ki}}{S_{mn}S_{nm}}, \tag{13}$$

where S_{ij} is the strain rate tensor [26,36]. This emergence of the third invariant of the symmetrized strain rate tensor is distinctly different from Smagorinsky's model for turbulent viscosity. Though physically appealing [37], further detailed numerical and theoretical analyses of the current framework are needed to establish usefulness of this approach for theoretical sub-grid modeling.

Finally, we conclude by highlighting the fact that entropic formulation of the continuous (in velocity space) BGK model provides a new discrete dynamical system analogue of Boltzmann dynamics. Thus, a Boltzmann-like framework extends the second law to discrete dynamical systems too.

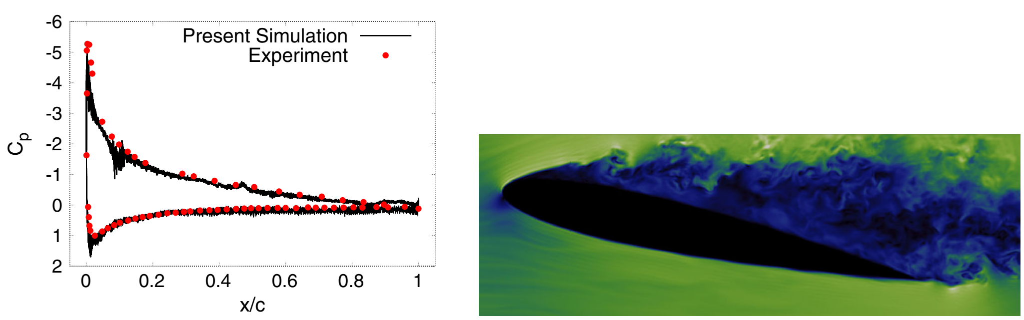

(a) C_p at AoA=10° and $Re = 2.88 \times 10^6$. (b) Visualization of stall at AoA=12° and $Re = 5 \times 10^4$

FIG. 5. Flow over the NACA-0012 airfoil.

The authors acknowledge helpful discussions with Prof. B. Boghosian, Prof. I. V. Karlin, and Prof. A. Wagner and support from Prof. V. Kumaran and Dr V. Y. Mudkavi. The authors thank CSIR-4PI(CMMACS) for providing computational resources under the memorandum of understanding with SankhyaSutra Labs. We also thank Mr. R. P. Thangavelu for ensuring continuous and smooth access to the cluster.

*ansumali@jncasr.ac.in

[1] S. Succi, *The Lattice Boltzmann Equation: For Fluid Dynamics and Beyond* (Oxford University Press, Oxford, 2001).
[2] I. V. Karlin, A. Ferrante, and H. C. Öttinger, Europhys. Lett. **47**, 182 (1999).
[3] S. Succi, I. V. Karlin, and H. Chen, Rev. Mod. Phys. **74**, 1203 (2002).
[4] N. Frapolli, S. S. Chikatamarla, and I. V. Karlin, Phys. Rev. Lett. **117**, 010604 (2016).
[5] A. Mazloomi M, S. S. Chikatamarla, and I. V. Karlin, Phys. Rev. Lett. **114**, 174502 (2015).
[6] M. Mendoza, B. M. Boghosian, H. J. Herrmann, and S. Succi, Phys. Rev. Lett. **105**, 014502 (2010).
[7] F. Fillion-Gourdeau, H. J. Herrmann, M. Mendoza, S. Palpacelli, and S. Succi, Phys. Rev. Lett. **111**, 160602 (2013).
[8] M. Mendoza, S. Succi, and H. J. Herrmann, Phys. Rev. Lett. **113**, 096402 (2014).
[9] L. Biferale, P. Perlekar, M. Sbragaglia, and F. Toschi, Phys. Rev. Lett. **108**, 104502 (2012).
[10] D. Vincenzi, P. Perlekar, L. Biferale, and F. Toschi, Phys. Rev. E **92**, 053004 (2015).
[11] M. Namburi, S. Krithivasan, and S. Ansumali, Sci. Rep. **6**, 27172 (2016).
[12] H. Chen, S. Chen, and W. H. Matthaeus, Phys. Rev. A **45**, R5339 (1992).
[13] Y. H. Qian, D. d'Humières, and P. Lallemand, Europhys. Lett. **17**, 479 (1992).
[14] G. R. McNamara and G. Zanetti, Phys. Rev. Lett. **61**, 2332 (1988).
[15] C. K. Aidun and J. R. Clausen, Annu. Rev. Fluid Mech. **42**, 439 (2010).
[16] R. Benzi, S. Succi, and M. Vergassola, Phys. Rep. **222**, 145 (1992).
[17] U. Frisch, B. Hasslacher, and Y. Pomeau, Phys. Rev. Lett. **56**, 1505 (1986).
[18] F. J. Higuera, S. Succi, and R. Benzi, Europhys. Lett. **9**, 345 (1989).
[19] B. M. Boghosian, J. Yepez, P. V. Coveney, and A. J. Wagner, Proc. R. Soc. A **457**, 717 (2001).
[20] S. Ansumali, I. V. Karlin, and H. C. Öttinger, Europhys. Lett. **63**, 798 (2003).
[21] I. V. Karlin, A. N. Gorban, S. Succi, and V. Boffi, Phys. Rev. Lett. **81**, 6 (1998).
[22] B. M. Boghosian, P. J. Love, P. V. Coveney, I. V. Karlin, S. Succi, and J. Yepez, Phys. Rev. E **68**, 025103 (2003).
[23] A. J. Wagner, Europhys. Lett. **44**, 144 (1998).
[24] H. Chen and C. Teixeira, Comput. Phys. Commun. **129**, 21 (2000).
[25] F. Tosi, S. Ubertini, S. Succi, and I. V. Karlin, J. Sci. Comput. **30**, 369 (2007).
[26] S. S. Chikatamarla, S. Ansumali, and I. V. Karlin, Phys. Rev. Lett. **97**, 010201 (2006).
[27] S. Ansumali and I. V. Karlin, J. Stat. Phys. **107**, 291 (2002).
[28] R. A. Brownlee, A. N. Gorban, and J. Levesley, Phys. Rev. E **75**, 036711 (2007).
[29] A. N. Gorban and D. Packwood, Phys. Rev. E **86**, 025701 (2012).
[30] P. L. Bhatnagar, E. P. Gross, and M. Krook, Phys. Rev. **94**, 511 (1954).
[31] S. Ansumali and I. V. Karlin, Phys. Rev. Lett. **95**, 260605 (2005).
[32] See Supplemental Material at http://link.aps.org/supplemental/10.1103/PhysRevLett.119.240602 for the mathematical details of the derivation.
[33] A. N. Gorban, I. V. Karlin, V. B. Zmievskii, and T. Nonnenmacher, Physica (Amsterdam) **231A**, 648 (1996).
[34] S. M. Hosseini, R. Vinuesa, P. Schlatter, A. Hanifi, and D. S. Henningson, Int. J. Heat Fluid Flow **61**, 117 (2016).
[35] N. Gregory and C. O'reilly, *Low-Speed Aerodynamic Characteristics of NACA 0012 Aerofoil Section, Including the Effects of Upper-Surface Roughness Simulating Hoar Frost* (HM Stationery Office, London, 1973).
[36] O. Malaspinas, M. Deville, and B. Chopard, Phys. Rev. E **78**, 066705 (2008).
[37] C. Meneveau, Annu. Rev. Fluid Mech. **43**, 219 (2011).